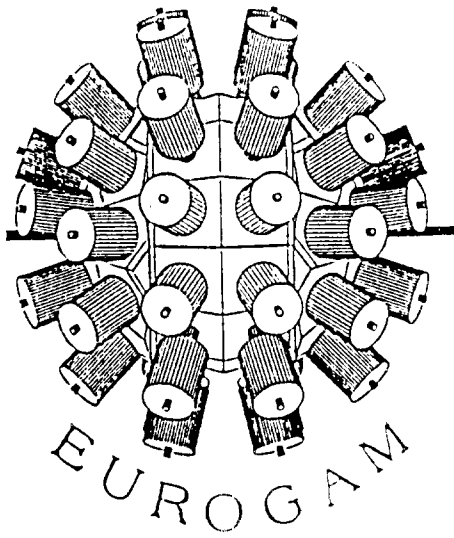


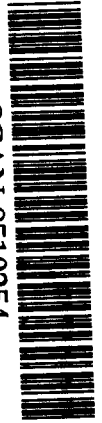
BB



FRANCE - UK

Collaboration

SCAN-9510254



CERN LIBRARIES, GENEVA

CRN 95-36

SCW 9544

Favoured neutron excitations in superdeformed ^{147}Gd .

Ch. Theisen¹, J.P. Vivien¹, I. Ragnarsson², C.W. Beausang³, F.A. Beck¹, G. Bélier^{1,9}, Th. Byrski¹, D. Curien¹, G. de France¹, D. Disdier¹, G. Duchêne¹, Ch. Finck¹, S. Flibotte⁴, B. Gall¹, B. Haas¹, H. Hanine⁵, B. Herskind⁶, B. Kharraja^{1,5,10}, J.C. Merdinger¹, A. Nourreddine⁵, B.M. Nyakó⁷, G.E. Perez⁷, S. Pilotte¹, D. Prévost¹, O. Stezowski¹, V. Rauch¹, C. Rigollet¹, H. Savajols¹, J. Sharpey-Schafer^{1,3,}, P.J. Twin³, L. Wei¹, K. Zuber⁸*

- ¹ Centre de Recherches Nucléaires et ULP, F-67037 Strasbourg Cedex 2, France
- ² Department of Mathematical Physics, Lund Institute of Technology, S-22100 Lund, Sweden.
- ³ Oliver Lodge Laboratory, University of Liverpool, Liverpool L69 3BX, UK
- ⁴ Department of Physics and Astronomy, McMaster University, Hamilton, Ontario, Canada M5S 1A7
- ⁵ Department of Physics, University Chouaib Doukkali, BP 20 El-Jadida, Morocco.
- ⁶ The Niels Bohr Institute, University of Copenhagen, Tandem Accelerator Laboratory, DK-4000 Roskilde, Denmark.
- ⁷ Institute of Nuclear Research, Bem tér 18/c, H-4001 Debrecen PF51, Hungary.
- ⁸ Institute of Nuclear Physics, Pl-342 Krakow, Poland.
- ⁹ Centre d'Etudes de Bruyères-le-Chatel, F-91680 Bruyères le Chatel, France
- ¹⁰ Department of Physics, Notre Dame University, Notre Dame, 46556 Indiana, USA.
- * Present address : National Accelerator Center, Cape Town, P.O. Box 72, ZA 7131, South Africa

Submitted to *Phys. Lett. B*

**CENTRE DE RECHERCHES NUCLEAIRES
STRASBOURG**

Favoured neutron excitations in superdeformed ^{147}Gd .

Ch.Theisen¹, J.P. Vivien¹, I.Ragnarsson², C.W.Beausang³, F.A.Beck¹, G.Belier^{1,9},
T.Byrski¹, D.Curien¹, G.de France¹, D.Disdier¹, G.Duchêne¹, Ch.Finck¹, S.Flibotte⁴,
B.Gall¹, B.Haas¹, H.Hanine⁵, B.Herskind⁶, B.Kharraja^{1,5,10}, J.C.Merdinger¹,
A.Nourreddine⁵, B.M.Nyakó⁷, G.E.Perez⁷, S.Pilotte¹, D.Prévost¹, O.Stezowski¹, V.Rauch¹,
C.Rigollet¹, H.Savajols¹, J.Sharpey-Schafer^{1,3,*}, P.J.Twin³, L.Wei¹, K.Zuber⁸

¹ *Centre de Recherches Nucléaires, F-67037, Strasbourg CEDEX 2, France.*

² *Department of Mathematical Physics, Lund Institute of Technology, S-22100 Lund, Sweden.*

³ *Oliver Lodge Laboratory, University of Liverpool, L69 3BX, United Kingdom.*

⁴ *Department of Physics and Astronomy, McMaster University, Hamilton, Ontario, Canada M5S*

1A7.

⁵ *Department of Physics, University Chouaib Doukkali, BP20 El-Jadida, Morocco.*

⁶ *The Niels Bohr Institute, University of Copenhagen, Tandem Accelerator Laboratory, DK-4000*

Roskilde, Denmark.

⁷ *Institute of Nuclear Research, Berm tér 18/c, H-4001 Debrecen PF51, Hungary.*

⁸ *Institute of Nuclear Physics, Pl-342 Krakow, Poland.*

⁹ *Centre d'Etudes de Bruyères-le-Chatel, F-91680, Bruyères le Chatel, France*

¹⁰ *Department of Physics, Notre Dame University, Notre Dame, 46556 Indiana, U.S.A.*

(August 3, 1995)

Abstract

Three new superdeformed (SD) bands have been observed in ^{147}Gd using the EUROGAM II spectrometer. Comparing to other $^{146,148,149}\text{Gd}$ SD bands,

*Present address : National Accelerator Center, Cape Town, P.O. Box 72, ZA 7131, South Africa

we use the effective alignment to assign excited band configurations, with the support of the Nilsson-Strutinsky cranking formalism. The effect of the crossing of the [642]5/2 and [651]1/2 neutron orbitals lying just below the magic $N = 86$ superdeformed shell gap has been investigated for the $^{146,147,148}\text{Gd}$ bands. Evidence for the presence of the [411]1/2 orbital is also given.

21.10.Re, 23.20.Lv, 27.60.+j

Predicted in the seventies and experimentally observed at very high spin in 1986 [1], superdeformed (SD) nuclei have triggered feverish activity in experimental and theoretical nuclear structure [2]. It was soon realized that high- j intruder orbitals play an important role [3]. In the $A \simeq 150$ mass region, the intruder orbitals originating from the $N = 7$ neutron or $N = 6$ proton oscillator shells approach the Fermi surface at large deformations and are strongly affected by Coriolis forces. Calculations based on the cranked shell correction method have explained many characteristics of the observed SD bands [4,5]. In particular, the smooth variations in the dynamical moments of inertia of yrast SD bands have been successfully interpreted in terms of different occupations of these high- N intruder states. With the increased sensitivity of the new generation of γ -ray spectrometer arrays, it has become possible to observe higher-lying SD bands. The information of these excited bands provides a sensitive test of the nucleon single-particle energy levels and in particular of non-intruder orbits predicted to lie near the Fermi surface at large deformation. With different filling of the non intruder neutron orbitals $[651]1/2$ and $[642]5/2$ $\alpha = \pm 1/2$ lying just below the $N = 86$ neutron SD shell gap, it has been possible to understand the observed features in the $\mathcal{J}^{(2)}$ moment of inertia of bands 1 and 2 in ^{147}Gd and their relation with the neighbouring isotopes $^{146-148}\text{Gd}$ [6,7]. In this letter we report on three new excited bands in the ^{147}Gd nucleus. The interpretation of these excited bands corresponds to a neutron excitation with the proton configuration remaining unchanged and provides evidence for the presence of the $[411]1/2$ Nilsson orbital lying close in energy to the $N = 6$ orbitals.

The ^{147}Gd nucleus has been investigated using the EUROGAM II array [8] installed at the Vivitron accelerator of the Centre de Recherches Nucléaires in Strasbourg. High spin states were populated via the $^{122}\text{Sn}(^{30}\text{Si},5n)^{147}\text{Gd}$ reaction at a beam energy of 158 MeV. Two stacked self-supporting ^{122}Sn targets, each $400\mu\text{g}/\text{cm}^2$ thick, were used with a ~ 3 pna ^{30}Si beam. The EUROGAM II spectrometer consists of 54 high efficiency Ge detectors (30 tapered coaxial detectors and 24 clover detectors) providing a photopeak efficiency of 7.4 % at 1.33 MeV. A condition of Ge fold ≥ 7 was required to accept an event into the data acquisition system. Only Compton suppressed Ge data were stored on tape and each event

had an additional condition that the suppressed Ge fold was ≥ 4 . A total of 1.8×10^9 events consisting of 700×10^6 γ^4 , 500×10^6 γ^5 , 250×10^6 γ^6 and 350×10^6 $\gamma^{>6}$ events were collected.

The data have been analysed using the “non-spiked” procedure described in [9]. A database established on the method described in [10] has been developed to store all events up to fold 20 in memory without unpacking.

Spectra of bands 1 and 2, previously reported in [11,6], have been produced by requiring that at least four gates be satisfied (i.e. events with fold ≥ 5). Using their clean high statistics spectra, the bands have been extended to higher frequency. Three new weaker SD bands have been found using an automatic search procedure implemented on the database [12] and which required three gates to be satisfied. Known γ -ray transitions between normally-deformed states in ^{147}Gd are observed in coincidence with the new SD intra-band transitions, showing that the bands can be unambiguously assigned to this nucleus. The γ -ray transition energies of the five bands labelled by order of their discovery are given in Table I. The intensities of the excited bands 2 to 5 relative to the yrast SD band are $50 \pm 5\%$, $17 \pm 5\%$, $25 \pm 5\%$ and $11 \pm 3\%$, respectively.

In the interpretation of the band structure, we use the effective alignment i_{eff} as defined in [6,7] and we compare for example the bands in ^{147}Gd with those in ^{148}Gd which have an additional neutron. If the spins of two bands are plotted as a function of frequency ω ($\hbar\omega = E_\gamma/2$), the effective alignment is simply the difference in spin between the two bands at a fixed frequency. The main contribution to i_{eff} is the alignment of the extra particle, but changes in deformation, pairing, etc. induced by this particle will also have some influence.

The effective alignment deduced from the observed bands is then compared with calculated values based on the Nilsson-Strutinsky cranking formalism with a modified oscillator potential [6,7] and in which pairing correlations are neglected. In this formalism, it is possible to fix different configurations and to follow their evolution when the spin changes.

Figure 1 is a schematic drawing of the single-particle orbitals active in ^{147}Gd (a realistic diagram of the calculated orbitals can be found in Ref. [6]). Starting from the orbitals oc-

cupied in the yrast band of ^{149}Gd , we indicate configurations assumed for the ^{148}Gd bands according to Ref. [13] and our proposal for the ^{147}Gd bands, proposal based in a first step on the behaviour of the $\mathcal{J}^{(2)}$ moment of inertia. From this diagram, it can be readily seen which bands can be compared to deduce i_{eff} . For example, the $^{148}\text{Gd}(1)$ band differs from the $^{149}\text{Gd}(1)$ band by a hole in the $[651]1/2$ $\alpha = 1/2$ orbital but it should be also noted that $^{147}\text{Gd}(1)$ differs from the $^{148}\text{Gd}(2)$ by a hole in the same orbital. Consequently, the effective alignment of this orbital can be obtained in two ways from experimental data and in each case compared with calculations. Using other bands as illustrated below, we obtain i_{eff} for the other orbitals of Fig. 1. We first note that, without any calculations, we can investigate if the values of i_{eff} for a suggested excitation are consistent among themselves when different pairs of bands are compared. When this is the case, it suggests that the same orbital is being filled. Comparison with i_{eff} theoretical calculations validates the suggested configurations as shown in Fig. 1.

One striking feature near the $N=83$ neutron Fermi surface is the interaction between the $[651]1/2$ and $[642]5/2$ negative signature orbitals at a rotational frequency $\hbar\omega \simeq 0.7$ MeV. When the orbital labeled $[642]5/2$ $\alpha = -1/2$ is full and the $[651]1/2$ $\alpha = -1/2$ orbital is empty, one expects a bump in $\mathcal{J}^{(2)}$. This is the case for the $^{147}\text{Gd}(1)$, $^{146}\text{Gd}(1)$ and $^{148}\text{Gd}(2)$ bands. In contrast, when both the $[651]1/2$ and $[642]5/2$ $\alpha = -1/2$ orbitals are occupied, the crossing of these two levels is “blocked”, resulting in a monotonic behaviour of the moment of inertia, as observed experimentally for the $^{147}\text{Gd}(2)$, $^{147}\text{Gd}(3)$ and $^{147}\text{Gd}(4)$ bands.

The moment of inertia of $^{147}\text{Gd}(5)$ also displays a bump. By comparing to the yrast band, we propose that it originates from removing a neutron from the $[411]1/2$ $\alpha = +1/2$ and filling the $[651]1/2$ $\alpha = +1/2$ orbital. One way to check this suggestion is to compare the crossing frequency corresponding to the position of the bump in the dynamical moment of inertia plot for the $^{147}\text{Gd}(1)$, $^{146}\text{Gd}(1)$, $^{148}\text{Gd}(2)$ and $^{147}\text{Gd}(5)$ bands, as displayed in Fig. 2. With increasing deformation, the energy gap between the $[651]1/2$ and $[642]5/2$ orbitals is reduced, pushing down the crossing frequency. The difference between the $^{147}\text{Gd}(1)$ and

$^{146}\text{Gd}(1)$ band configurations is one neutron in the $[642]5/2 \alpha = +1/2$ orbital which, because of compensating ϵ_2 and ϵ_4 deformation effects, has little influence on the crossing frequency. These two bands therefore exhibit the same pattern. Compared to $^{147}\text{Gd}(1)$, the $^{148}\text{Gd}(2)$ configuration corresponds to an additional neutron in the $[651]1/2 \alpha = +1/2$ orbital. Filling this deformation driving orbital leads to a lower crossing frequency. Band 5 corresponds to a hole in the $[411]1/2 \alpha = +1/2$ as compared to $^{148}\text{Gd}(2)$. Removing the contribution of this orbital also increases the deformation, shifting down the crossing frequency. An additional check of the proposed configurations is to investigate the effective alignment of the $[651]1/2 \alpha = -1/2$ orbital, as displayed in Fig. 3a. The calculated alignment of $^{147}\text{Gd}(5)$ relative to $^{148}\text{Gd}(6)$ is in good agreement with experiment. The disagreement observed between the calculated and experimental alignment of $^{148}\text{Gd}(2)$ relative to $^{149}\text{Gd}(1)$ has been suggested [14] as evidence of pairing correlations present in ^{149}Gd which are not included in the present calculations.

Band 3 exhibits a relatively low moment of inertia and a sharp rise at high rotational frequency. Similar features have already been observed in $^{148}\text{Gd}(3)$ [13]. The proposed configuration involves at low rotational frequency the excitation of the neutron from the $[770]1/2 \alpha = -1/2$ orbital to the $[651]1/2 \alpha = -1/2$ orbital. This configuration blocks the $N = 6$ band crossing and the observed low moment of inertia corresponds to the $\nu 7^0$ intruder configuration. This assumption is supported when we compare the effective alignment of the $[651]1/2 \alpha = +1/2$ and $[770]1/2 \alpha = -1/2$ orbitals respectively. In Fig. 3b, the effective alignment deduced from $^{147}\text{Gd}(3)$ relative to $^{148}\text{Gd}(3)$, $^{147}\text{Gd}(2)$ relative to $^{148}\text{Gd}(4)$, $^{148}\text{Gd}(1)$ relative to $^{149}\text{Gd}(1)$ and the calculated one which corresponds to the alignment of the $[651]1/2 \alpha = +1/2$ orbital are displayed. We also show in Fig. 3c the effective alignment of $^{148}\text{Gd}(3)$ relative to $^{149}\text{Gd}(1)$ and $^{147}\text{Gd}(3)$ relative to $^{148}\text{Gd}(1)$, both assumed to correspond to the $[770]1/2 \alpha = -1/2$ orbital. The high values calculated agree reasonably well with experiment. Note, however, that this agreement is obtained only for specific relative spin assignments (see Table I) where at a fixed frequency, the spin values of band 3 are

considerably lower than for the other bands. This assumption is confirmed by the fact that the $^{147}\text{Gd}(3)$ band decays to normally deformed states with energies and spins similar to those of $^{147}\text{Gd}(1)$. The sharp rise observed at the highest frequency could originate from an interaction between the $N = 7$ and $N = 5$ orbitals.

The $^{147}\text{Gd}(4)$ band has transition energies identical to the threequarter-point energies of $^{148}\text{Gd}(1)$ to within 2 keV. This identity can be obtained if the configuration of $^{147}\text{Gd}(4)$ corresponds to the $^{148}\text{Gd}(1)$ band configuration with a neutron hole in an orbital with zero alignment. Increasing the deformation, the $[411]1/2$ orbital comes closer to the Fermi surface and becomes the most favoured candidate. Calculations of the effective alignment and dynamical moment of inertia of promoting a neutron from $[411]1/2 \alpha = +1/2$ to the $[651]1/2 \alpha = -1/2$ orbital fit the experimental values observed for this band (see Fig. 3d). The excitation of the same orbital was also proposed for $^{148}\text{Gd}(6)$ which has energies at the threequarter-points of $^{149}\text{Gd}(1)$ [15]. The absence in our data of a band which can be assigned to the other signature partner of the $[411] 1/2$ orbital suggests a significant signature splitting of this orbital in the feeding region. Very recently [16], an excited band (band 4) has been discovered in ^{151}Dy . It is characterized by a $\mathcal{J}^{(2)}$ moment of inertia similar to that of the $^{152}\text{Dy}(1)$ band and is in marked contrast to the $\mathcal{J}^{(2)}$ behaviour of the yrast band of ^{151}Dy . The transition energies of this new band are very close to the half-point energies of $^{152}\text{Dy}(1)$ and result in an effective alignment close to $0.5(\text{mod}1)\hbar$. It has been proposed [16] that this band may also be associated with the $[411]1/2 \alpha = +1/2$ orbital which in the pseudo-coupling scheme has a half integer alignment. It remains however to be seen whether the larger deformation attributed to $^{151}\text{Dy}(4)$ can account for the difference in slope of the $[411]1/2 \alpha = +1/2$ orbital which seems to be close to zero in the lighter $^{147,148}\text{Gd}$ isotopes.

In summary, three new SD bands interpreted as neutron excitations have been found in ^{147}Gd . Combined with the two bands reported previously in the same nucleus, the six bands

in ^{148}Gd and the yrast SD bands in ^{146}Gd and ^{149}Gd , they form an excellent data set to identify the neutron Nilsson orbitals present below the $N = 86$ neutron superdeformed shell gap. Thus, when comparing different pairs of bands, we find similar effective alignments (see Fig. 3) in many cases. This leads further support to previous interpretations [17,6] of which orbitals are being filled in going from a band in nucleus A to a band in isotope $A+1$. For example, we now conclude that the orbital being filled when forming the $^{149}\text{Gd}(1)$ band from the $^{148}\text{Gd}(1)$ band is also being filled when forming the $^{148}\text{Gd}(4)$ band from the $^{147}\text{Gd}(2)$ band and the $^{148}\text{Gd}(3)$ band from the $^{147}\text{Gd}(3)$ band (see Figs. 1 and 3b). This conclusion is independent of the specific Nilsson orbital. Comparisons with calculations, however, suggest that it is the $[651] 1/2 \alpha = +1/2$ orbital which is active. Considering all the bands, a consistent picture emerges where the active orbitals are $[651]1/2 \alpha = \pm 1/2$, $[642]5/2 \alpha = +1/2$ and $[411]1/2 \alpha = +1/2$. (In the $^{146}\text{Gd}(2)$ band, the $[642]5/2 \alpha = -1/2$ orbital is active [6,7]). A very important factor for our interpretation is the crossing between the two $N = 6$, $\alpha = -1/2$ orbitals which changes in frequency among different bands as expected from the calculated differences in deformation. Finally, as for the $^{148}\text{Gd}(3)$ band and essentially independent of the interpretation for the other bands, we get a reasonable agreement between calculation and experiment if the lowest $N = 7$ orbital is emptied in the $^{147}\text{Gd}(3)$ band.

EUROGAM is funded jointly by the EPSRC (U.K.) and the IN2P3 (France). K.Z. is supported by the Polish KBN Grant, No. 2 P03B 121 08. This work was supported in part by the Swedish Natural Science Research Council. G.E.P. and B.M.N. acknowledge support from Hungarian Scientific Research Fund OTKA No. 3017.

TABLES

TABLE I. Gamma-ray transition energies (keV) and statistical uncertainties (in parentheses) for the different SD bands in ^{147}Gd discussed in the present work. Assuming the spin sequence $29.5 \rightarrow 27.5$ for the lowest transition observed in band 1, then the corresponding sequences for band 2 to 5 are : $32.5 \rightarrow 30.5$, $27.5 \rightarrow 25.5$, $32.5 \rightarrow 30.5$, $37.5 \rightarrow 35.5$.

band 1	band 2	band 3	band 4	band 5
697.04 (05)	730.21 (12)	704.8 (5)	741.9 (4)	899.5 (4)
745.31 (06)	778.94 (08)	753.1 (2)	785.5 (4)	951.1 (3)
795.53 (06)	828.02 (08)	803.8 (2)	834.4 (3)	994.0 (2)
847.03 (06)	877.74 (07)	857.0 (1)	883.7 (3)	1036.1 (2)
899.95 (07)	929.02 (07)	910.7 (1)	935.9 (2)	1079.7 (3)
954.36 (07)	981.60 (08)	966.4 (1)	988.6 (2)	1125.6 (2)
1009.55 (07)	1035.49 (08)	1022.7 (1)	1042.0 (2)	1174.5 (2)
1065.24 (06)	1090.42 (08)	1080.2 (1)	1096.9 (2)	1223.1 (3)
1121.03 (07)	1146.67 (08)	1137.6 (1)	1153.5 (2)	1272.8 (3)
1175.45 (08)	1203.52 (09)	1195.3 (1)	1209.5 (2)	1323.1 (3)
1228.44 (07)	1261.38 (09)	1253.0 (2)	1267.7 (2)	1374.3 (3)
1277.52 (09)	1320.44 (10)	1310.7 (2)	1326.1 (3)	1428.0 (4)
1323.14 (09)	1380.04 (12)	1367.7 (2)	1384.4 (3)	1484.1 (6)
1367.21 (11)	1439.81 (13)	1423.2 (2)	1443.6 (3)	
1413.74 (11)	1500.33 (16)	1477.3 (3)	1502.7 (5)	
1463.77 (16)	1561.34 (24)	1522.7 (3)	1563.4 (7)	
1516.33 (23)	1622.84 (40)	1512.2 (7)		
1571.88 (29)				
1627.76 (66)				

REFERENCES

- [1] P.J.Twin *et al.*, Phys. Rev. Lett. **57** 811 (1986).
- [2] R.V.J.Janssens and T.L.Khoo, Annu. Rev. Nucl. Part. Sci. **41** 321 (1991).
M. Meyer and J.P.Vivien, Ann. Phys. (Paris) **17** 11 (1992).
- [3] I.Ragnarsson and S.Åberg, Phys. Lett. B **180** 191 (1986).
- [4] T.Bengtsson, I.Ragnarsson and S.Åberg, Phys. Lett. B **208** 39 (1988).
- [5] W.Nazarewicz, R.Wyss and A.Johnson, Nucl. Phys. **A503** 285 (1989).
- [6] B.Haas *et al.*, Nucl. Phys. **A561** 251 (1993).
- [7] I.Ragnarsson, Nucl. Phys. **A557** 167c (1993).
- [8] C.W. Beausang *et al.*, Nucl. Instrum. Meth. Phys. Res. **A313** 37 (1992);
F.A.Beck, Prog. Part. Nucl. Phys. **28** 443 (1992).
- [9] C.W. Beausang *et al.*, to appear in Nucl. Instrum. Meth. Phys. Res.
- [10] S.Flibotte *et al.*, Nucl. Instrum. Meth. Phys. Res. **A320** 325 (1992).
- [11] K.Zuber *et al.*, Phys. Lett. B **254** 308 (1991).
- [12] Ch.Theisen, Ph.D. Thesis, CRN 95-12.
- [13] G.de France *et al.*, submitted to Phys. Lett. B.
- [14] G.de France *et al.*, Phys. Lett. B **331** 290 (1994).
- [15] S.Flibotte *et al.*, Nucl. Phys. **A584** 373 (1995).
- [16] D.Nisius *et al.*, Phys. Lett. B **346** 15 (1995).
- [17] I.Ragnarsson, Phys. Lett. B **264** 5 (1991).

FIGURES

FIG. 1. Schematic routhians.

Various configurations of ^{148}Gd and ^{147}Gd SD bands are plotted relative to the yrast band of ^{149}Gd . Empty circles correspond to holes in the yrast band of ^{149}Gd . Solid (dotted) curves indicate $\pi = +, \alpha = +1/2$ ($\pi = +, \alpha = -1/2$). The dot-dashed (dashed) curve indicates $\pi = -, \alpha = -1/2$ ($\pi = -, \alpha = +1/2$). For $^{147}\text{Gd}(3)$ and $^{148}\text{Gd}(3)$, the indicated configurations correspond to rotational frequencies below the sharp rise in moment of inertia. $^{148}\text{Gd}(5)$ is the only case where the $[770]1/2 \alpha = +1/2$ orbital is filled.

FIG. 2. Calculated (upper part) and experimental (lower part) dynamical moments of inertia.

FIG. 3. Calculated effective alignment values for the following neutron orbitals a) $[651]1/2 \alpha = -1/2$ orbital, b) $[651]1/2 \alpha = +1/2$ orbital, c) $[770]1/2 \alpha = -1/2$ orbital, d) $[411]1/2 \alpha = +1/2$ orbital. In the lower part of each panel are represented the experimental i_{eff} values deduced when comparing specific bands. The experimental data for $^{147}\text{Gd}(3)$ and $^{148}\text{Gd}(3)$ are taken only below the sharp rise in moment of inertia.

Fig. 1

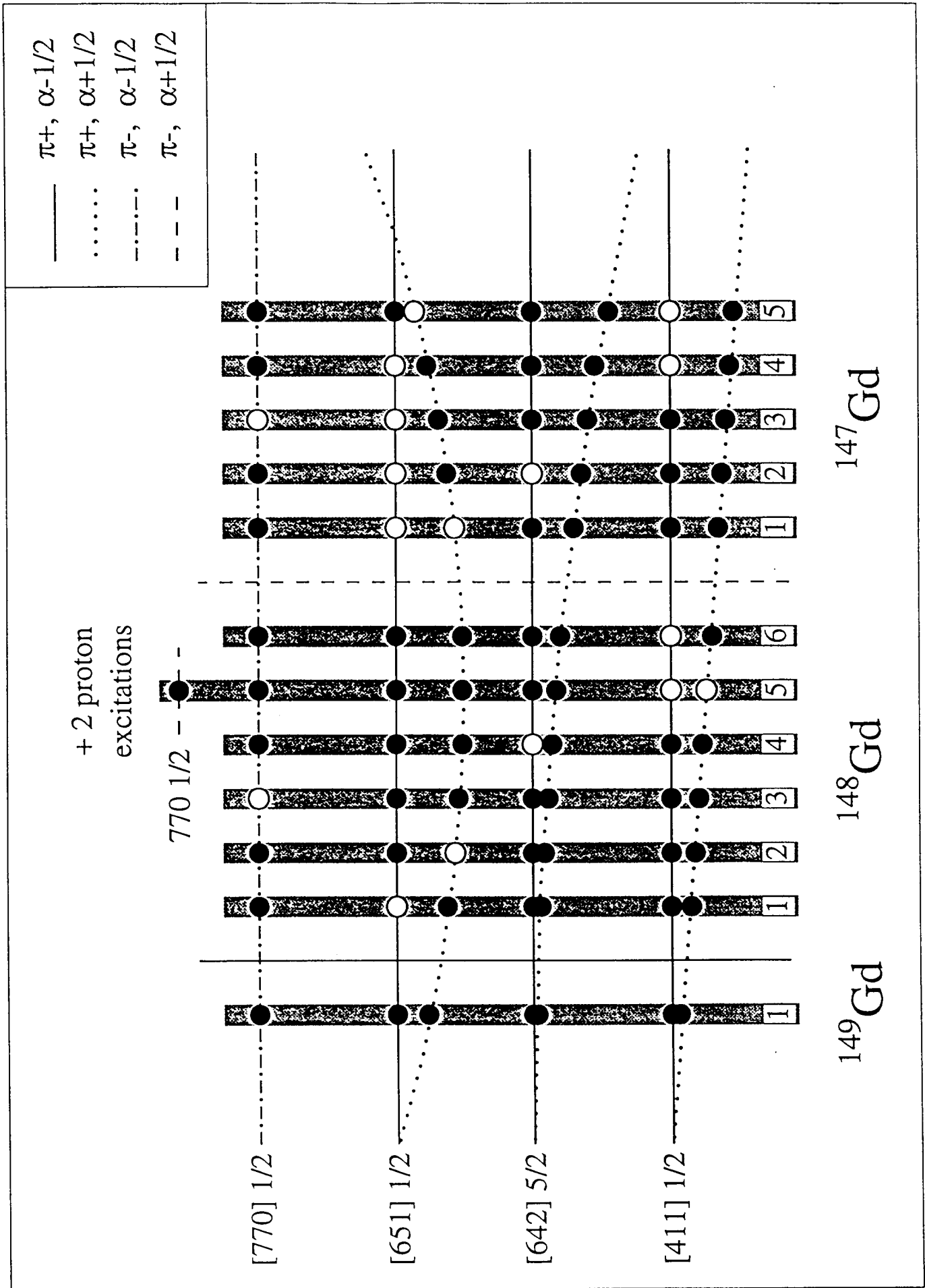


Fig. 2

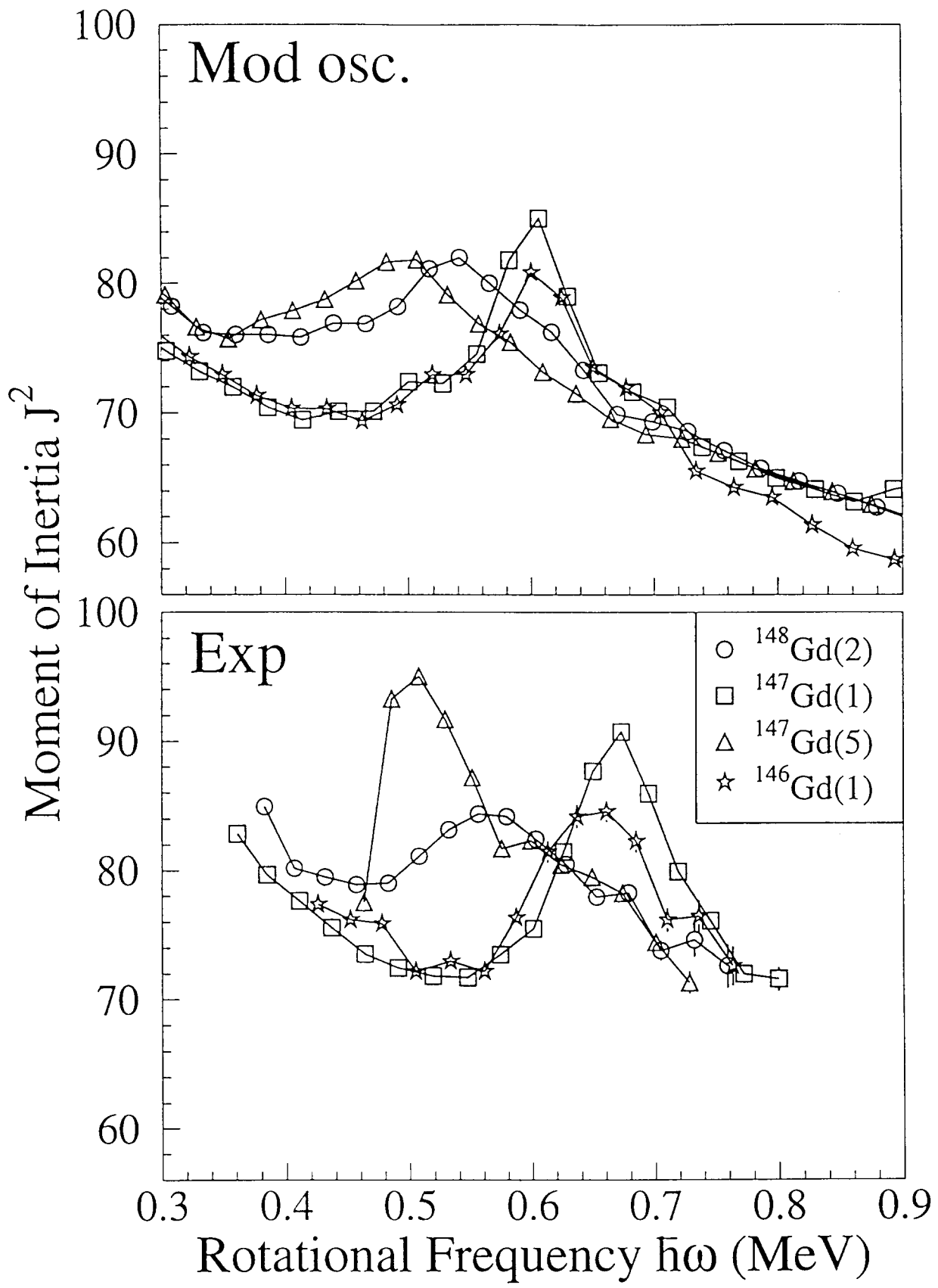
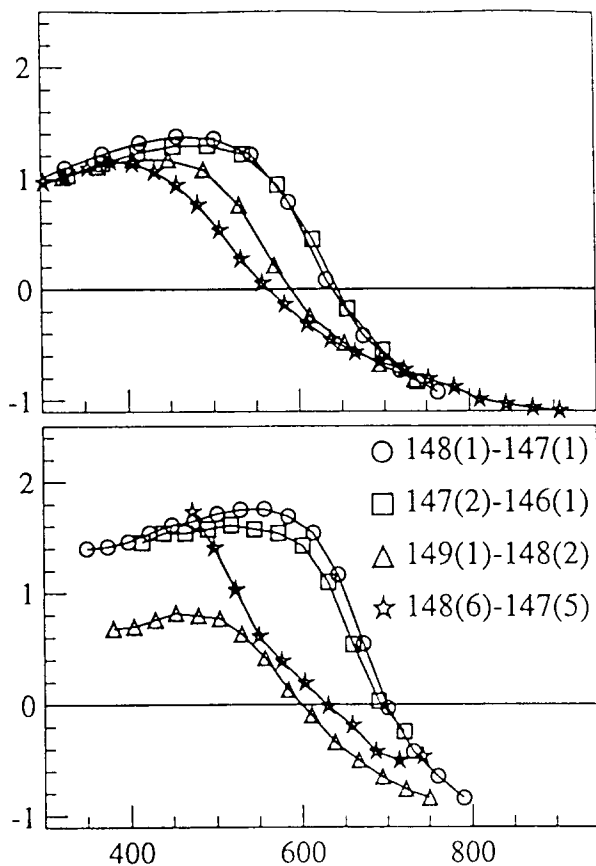


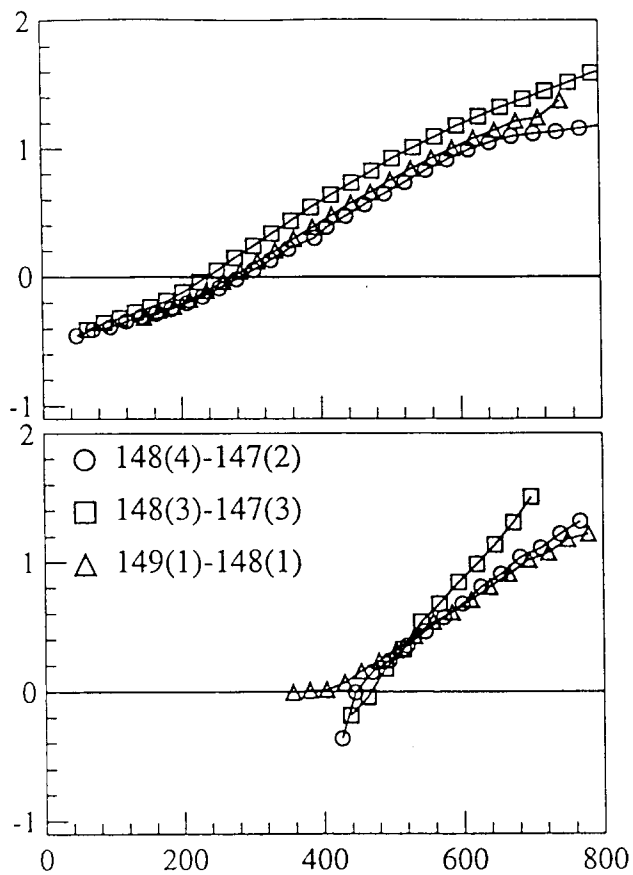
Fig. 3

Effective Alignment (\bar{h})

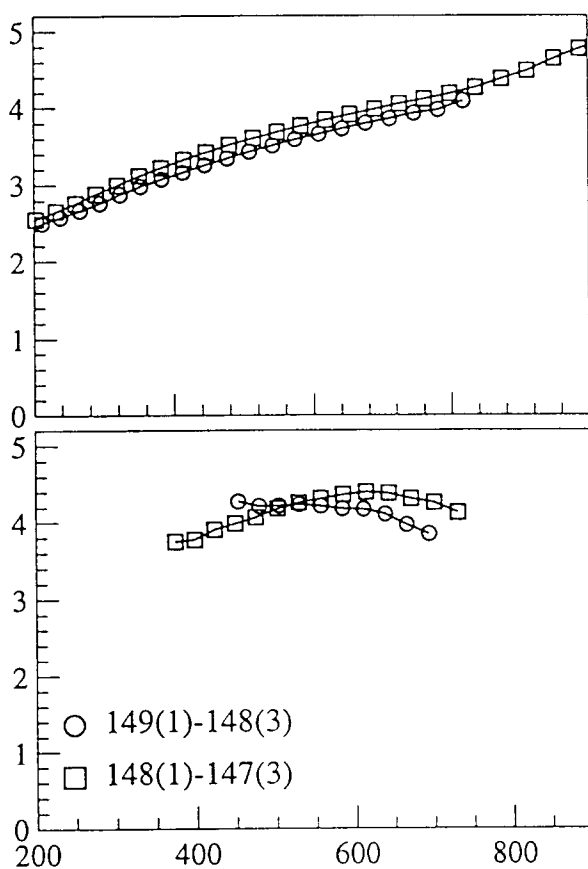
a) $[651]1/2 \alpha=-1/2$



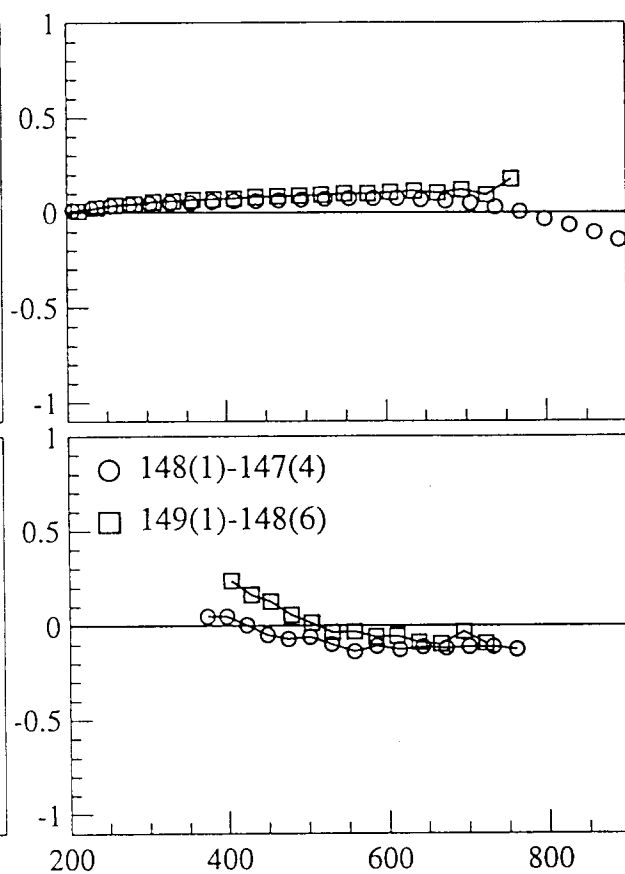
b) $[651]1/2 \alpha=+1/2$



c) $[770]1/2 \alpha=-1/2$



d) $[411]1/2 \alpha=+1/2$



Rotational Frequency (keV)

